

Antibody fragment immobilization on a planar gold and gold nanoparticle modified quartz crystal microbalance with dissipation sensor surfaces for immunosensor applications†

Cite this: DOI: 10.1039/c4ay00070f

A. Makaraviciute,^a T. Ruzgas,^b A. Ramanavicius^{cd} and A. Ramanaviciene^{*a}

Immunosensors are bioaffinity sensors incorporating immune system molecules that are utilized for analyte recognition and signal transduction yielding a measurable signal upon analyte detection. A lot of effort has been made to optimize the immobilization matrix on the sensor surface since the outcome of the ligand immobilization procedure determines sensitivity, specificity and longevity of the developed immunosensor. In this work, antibodies against bovine leukemia virus antigen gp51 were chemically reduced to "half" antibody fragments that were later employed as recognition ligands. Antibody fragments at different concentrations were immobilized *via* thiolate bonds on planar gold and gold nanoparticle modified surfaces of a quartz crystal microbalance with a dissipation sensor. Antibody fragment immobilization and interaction with antigens were investigated. Antibody fragment surface mass densities after the immobilization on planar gold and gold nanoparticle modified sensor surfaces were directly dependent on the initial antibody concentration. The highest analytical response was exhibited by antibody fragments immobilized at the smallest surface mass density on planar gold and gold nanoparticle modified surfaces. Bovine leukemia virus antigen gp51 interaction with antibody fragments was compared with non-specific gp51 interaction with bovine serum albumin on planar gold and gold nanoparticle modified surfaces by employing $\Delta D/\Delta f$ plots.

Received 8th January 2014
Accepted 16th January 2014

DOI: 10.1039/c4ay00070f

www.rsc.org/methods

1. Introduction

An immunosensor is a device providing analytical information. It is based on an immune system element functioning as a recognition molecule, which is in contact with a signal transducer. The main performance characteristics of an immunosensor including sensitivity, specificity, and reusability depend predominantly on the ligand immobilization technique and the resulting interface between the immobilized capture ligands and the sample solution containing analyte molecules. When antibodies are used as capture ligands, it is crucial to consider the effect of the immobilization technique on antibody activity, paying special attention to orientation and

stability as the performance of the immobilized antibodies largely depends on these features.¹ It has been shown^{2–4} that antibody orientation has a significant effect on their functionality, and a number of immobilization techniques have been proposed enabling site-directed antibody orientation on the sensor surface, for example, employing the Fc binding proteins,⁵ oxidising oligosaccharide moieties⁶ and producing antibody fragments (Frag-Ab) with free sulfhydryl groups that are exposed after the reduction of disulfide bridges present in the hinge region.⁷

The surface preparation technique based on chemical reduction of antibody disulfide bridges is rapid, convenient, inexpensive and enables the formation of a well-oriented antibody layer immobilized *via* very stable bonds between the sulfhydryl groups and the gold surface (Au).⁸ However, it has been suggested that proteins might denature upon close contact with Au, which could result in a decreased performance of the immunosensor.⁹ Immobilizing antibodies on gold nanoparticles (AuNPs) might be a possible solution as by using model systems it has been demonstrated that globular proteins retain their structure better on higher curvature surfaces.^{10,11} Besides the potentially beneficial surface topography, AuNPs have an additional advantage of increased surface areas in comparison to planar Au surfaces and might result in a bigger

^aDepartment of Analytical and Environmental Chemistry, Faculty of Chemistry, Vilnius University, Naugarduko st 24, LT-03225 Vilnius, Lithuania

^bDepartment of Biomedical Sciences, Faculty of Health and Society, Malmö University, SE-20506 Malmö, Sweden

^cDepartment of Physical Chemistry, Faculty of Chemistry, Vilnius University, Naugarduko st 24, LT-03225 Vilnius, Lithuania

^dDepartment of Materials Science and Electronical Engineering, Semiconductor Physics Institute, State Scientific Research Institute Centre for Physical Sciences and Technology, A. Gostauto st 11, LT-01108 Vilnius, Lithuania

† Electronic supplementary information (ESI) available. See DOI: 10.1039/c4ay00070f

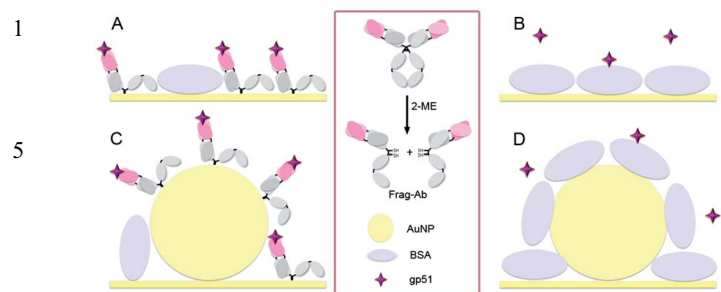


Fig. 1 Schematic representation of the experimental setup. A – gp51 interaction with Frag-Ab immobilized on the planar Au electrode surface; B – non-specific gp51 interaction with BSA adsorbed on the planar Au electrode surface; C – gp51 interaction with Frag-Ab immobilized on the AuNP modified Au electrode surface; D – non-specific gp51 interaction with BSA adsorbed on the AuNP modified Au electrode surface. Frag-Ab – fragmented (reduced at the hinge region) antibodies against gp51; AuNP – gold nanoparticles; BSA – bovine serum albumin, gp51 – bovine leukemia virus antigen.

surface density of recognition ligands which, in turn, could yield a subsequently higher response to antigens.¹²

The quartz crystal microbalance (QCM) is a piezoelectric surface sensitive technique that has been widely used in biosensor design.^{13–15} Although initially QCM had been developed for thin rigid film measurements, it was later developed for the evaluation of the surface bound protein layers. Conventional QCM registers quartz crystal resonance frequency change upon protein deposition on the surface and the new modification entitled quartz crystal microbalance with dissipation (QCM-D) enables the registration of the *D*-factor, which is related to energy dissipation caused by friction and viscoelastic properties of the layer. Although the mass of thin and rigid layers can be obtained from the QCM data using a linear frequency change-deposited mass dependence described by a Sauerbrey relation, the more bulky protein layers with trapped water are not as easily described. The main advantage of QCM-D is that this technique allows calculation of mass adsorbed on the surface more precisely than the conventional QCM and additionally enables the evaluation of viscoelastic properties and the water content of the protein layer.^{16,17} Hence, QCM-D data provide substantial information on the structure of the immunosensor interfaces and reaction parameters of the immobilized molecules.

In the present study, Frag-Ab immobilization and the resulting response to antigens on the planar QCM-D sensor surface and on AuNP modified sensor surfaces were analysed by the QCM-D method using a model system of bovine leukemia virus antigen gp51 (gp51) and specific antibodies against gp51. In addition, Frag-Ab/gp51 interaction and the non-specific bovine serum albumin (BSA) and gp51 interactions on planar and AuNP modified surfaces have been compared by the use of QCM-D $\Delta D/\Delta f$ plots (Fig. 1).

2. Experimental

2.1 Materials

2-Mercaptoethanol (2 ME), acetic acid, ammonium sulfate, bovine serum albumin, ethanol, gold(III) chloride hydrate,

hydrochloric acid, poly-L-lysine (PLL), potassium chloride, potassium hydrogen phosphate, sodium chloride, disodium hydrogen phosphate, and trisodium citrate dihydrate were obtained from Sigma-Aldrich, Germany. Lyophilized bovine leukemia virus antigen gp51 and serum enriched with specific antibodies against gp51 were purchased from BIOK, Russia. Gold-coated QCM-D quartz crystals (QSX 301) with a resonance frequency of 4.95 MHz and a diameter of 14 mm were obtained from Q-Sense AB, Sweden. Unstained Protein Molecular Weight Marker was purchased from ThermoFisher Scientific, USA.

2.2 Methods

2.2.1 AuNP synthesis. AuNP synthesis was carried out according to the method described by Turkevich *et al.*¹⁸ Briefly, 50 mL of 1 mM gold(III) chloride hydrate solution was heated under stirring until 90 °C was reached. Then, 2.308 mL of 1% trisodium citrate dehydrate was added and the mixture was incubated at 90 °C for 15 min while stirring and for 10 min with the stirring switched off. Afterwards the resulting AuNP colloid was allowed to cool down to room temperature and was subsequently dialyzed against deionized water (1 : 500) at +4 °C. The synthesized AuNPs were evaluated by TEM analysis, which revealed that the average size of AuNPs was 50 nm. When not in use, the AuNP colloid was stored at +4 °C.

2.2.2 Antibody precipitation. Polyclonal antibodies against gp51 were precipitated by mixing 10 mL of serum with an equivalent amount of saturated ammonium sulfate solution and incubating overnight at +4 °C under stirring. The mixture was then centrifuged at 5000 rpm for 20 min and the pellet was resuspended in 5 mL 10 mM phosphate buffered saline (PBS) pH 7.4. The resulting suspension was mixed with 5 mL of saturated ammonium sulfate solution and the precipitation step was repeated. After reconstitution, the antibody solution was dialyzed against 10 mM PBS pH 7.4 overnight at +4 °C. The protein concentration was evaluated spectrophotometrically according to the method described by Ehresmann *et al.*¹⁹ All solutions were prepared in UHQ water (conductivity less than 1 $\mu\text{S cm}^{-1}$) purified using a DEMIWA rosa (WATEK, Czech Republic).

2.2.3 Antibody reduction. In order to immobilize antibodies directly on the Au surface, sulfhydryl groups must become accessible. This was achieved by chemical reduction of disulfide bridges present in the antibody hinge region by 2 ME as described in our previous publication.³

Briefly, 37.5 μL of antibody suspension was mixed with 210 μL of 0.1 M 2 ME and 52.5 μL of 10 mM PBS pH 7.4 and incubated at 37 °C for 90 min. This procedure results in two identical “half” antibody fragments, *i.e.*, fragmented antibodies.^{2,20} Frag-Ab solutions were prepared from antibody solutions of three different concentrations of 100, 200 and 440 $\mu\text{g mL}^{-1}$.

2.2.4 Preparation of Frag-Ab modified planar Au QCM-D sensor surface. A QCM-D planar Au sensor with a resonance frequency of 4.95 MHz was rinsed with ethanol and deionised water and dried with nitrogen. It was then plasma cleaned (Harrich plasma cleaner PDC-32 G, Harrick Plasma, USA) for 10 min. Analysis was carried out using a Q-Sense E1 instrument

(Q-Sense AB, Sweden). Measurements were performed at 25 °C after recording a stable baseline. All solutions were degassed before use. The association steps were carried out in flow mode at 100 $\mu\text{L min}^{-1}$ flow speed and the dissociation steps were carried out at 200 $\mu\text{L min}^{-1}$.

Frag-Ab immobilization was carried out until saturation was reached. Then, the dissociation step was carried out for 10 min by rinsing the surface with buffer. After Frag-Ab immobilization the sensor surface was exposed to 10 mg mL^{-1} BSA following the protocol that was used for Frag-Ab deposit.

2.2.5 Preparation of Frag-Ab and AuNP modified QCM-D sensor surface. The QCM-D sensor was cleaned and mounted for analysis according to the same procedure as in the case of using a planar Au surface. After obtaining a stable baseline, the sensor surface was exposed to 0.002% PLL solution for 5 min in order to obtain a positively charged layer on the gold surface. Then, the surface was rinsed with deionized water for 10 min and subsequently AuNPs were electrostatically adsorbed from a colloid with 10 mM NaCl until equilibrium was reached. Afterwards the surface was rinsed with deionised water for 10 min, followed by 10 mM PBS pH 7.4 for 1 min. Finally, the surface was exposed to Frag-Ab and BSA as described previously.

2.2.6 Measurement of specific Frag-Ab/gp51 interactions. The prepared surface was exposed to a range of different concentrations of gp51 (0.01, 0.05, 0.1, 0.5 and 1 mg mL^{-1}). Each association phase was carried out for 30 min followed by a dissociation phase of 10 min. The interaction times were selected as a compromise between enough time to register a distinguishable analytical signal and the most rapid analysis time.

2.2.7 Measurement of non-specific BSA/gp51 interaction. BSA/gp51 interactions were measured on planar Au and AuNP modified surfaces. The QCM-D sensor was cleaned and mounted for analysis according to the same procedure as described previously. AuNP adsorption was carried out according to the protocol described above. BSA was pre-adsorbed on both planar Au and AuNP modified surfaces until a stable baseline was reached. Then, the prepared surface was allowed to react with 0.5 mg mL^{-1} gp51. The association phase was carried out for 30 min followed by a dissociation phase for 10 min.

2.2.8 Data processing. All experiments were performed at a minimum of three repetitions and the obtained data were processed using a QSoft program (Q-Sense, Sweden).

3. Results and discussion

In the present study antibodies against gp51 were reduced at their hinge region by 2 ME to yield Frag-Ab with free sulfhydryl groups. Frag-Ab were immobilized in a site-directed manner *via* sulfhydryl groups on planar Au and AuNP modified QCM-D electrode surfaces. The immobilization efficiency and response to gp51 of different systems were compared. Additionally, Frag-Ab/gp51 and non-specific interactions were evaluated (Fig. 1).

3.1 Antibody reduction

Frag-Ab reduction with 2 ME was performed using antibody solutions of three different concentrations of 100, 200 and 440

$\mu\text{g mL}^{-1}$. Reduction conditions were determined experimentally and the results were confirmed by SDS-PAGE analysis under non-reducing conditions (ESI Fig. S1†).

The Frag-Ab were positioned between 66.2 and 116 kDa marker bands and this was in good agreement with an approximate “half” Frag-Ab molecular weight of approx. 80 kDa considering that under the reducing conditions the heavy chain runs at 55 kDa and the light chain runs at 25 kDa. The response of Frag-Ab *vs.* the intact antibody to antigen gp51 was compared in our previous work. It has been shown that Frag-Ab exhibit better analytical signals for biosensing applications.³

3.2 Frag-Ab immobilization

After the reduction Frag-Ab were immobilized on planar Au and AuNP modified QCM-D electrode surfaces. Frag-Ab immobilization induced changes in QCM-D resonant frequency were converted to surface mass densities by the Sauerbrey relation.

Although *D*-factor values were relatively high suggesting the consideration of calculations based on the viscoelastic Voigt model, there were several motives in favour of using the Sauerbrey equation. Firstly, the use of the Sauerbrey equation significantly simplified the evaluation of the experimental data. Secondly, these calculations resulted in qualitatively correct evaluation of the overall kinetics and general tendencies of different system characteristics. Thirdly, the investigated layers are in the range of the QCM-D-excited shear wave extinction depth into the aqueous protein solution (~ 250 nm). This is the layer thickness range where the Sauerbrey relation is most likely to hold even for a viscoelastic layer.¹⁷

The Δf changes were calculated from the average of Δf responses of the 3rd, 5th, and 7th overtones. This approach has been chosen in an attempt to obtain data comparable to those acquired following fitting to a model since conventional fitting procedures include overtones mentioned above. For each process, two report points were chosen at 200 s prior to the adsorption phase and at 200 s prior to the end of the dissociation phase. The Δf changes were converted to surface mass densities by the Sauerbrey relation:

$$\Delta m = -\frac{C \times \Delta f}{n}$$

where *C* is 17.7 $\text{ng Hz}^{-1} \times \text{cm}^2$ for a 5 MHz quartz crystal and *n* is the overtone number. The results are presented in Table 1.

As can be seen from Table 1, the obtained results show that the surface mass densities of Frag-Ab immobilized on planar Au were directly dependent on the initial concentrations of antibody solutions. The highest surface mass density of 1378 ng cm^{-2} was observed in the case of Frag-Ab immobilization from antibody solution of 440 $\mu\text{g mL}^{-1}$ and the lowest surface mass density (922 ng cm^{-2}) was calculated after Frag-Ab immobilization from antibody solution of 100 $\mu\text{g mL}^{-1}$.

Up to 49% higher surface densities were registered by immobilizing Frag-Ab on AuNP modified surfaces. However, the comparison of planar Au and AuNP based systems was made difficult by the fact that the AuNP immobilization step exhibited relatively high dispersion of the results due to not fully

Table 1 QCM-D frequency change (Δf) and surface mass density (Γ) dependence on the initial antibody solution concentration. Frag-Ab – fragmented (reduced at the hinge region) antibodies against gp51, Au – planar gold, and AuNPs – gold nanoparticles

	Initial antibody solution concentration ($\mu\text{g mL}^{-1}$)					
	100		200		440	
	Δf (Hz)	Γ (ng cm^{-2})	Δf (Hz)	Γ (ng cm^{-2})	Δf (Hz)	Γ (ng cm^{-2})
Frag-Ab on Au	-52 ± 1	922 ± 24	-58 ± 2	1030 ± 33	-77 ± 3	1378 ± 53
Frag-Ab on AuNP	-101 ± 3	1807 ± 57	-103 ± 4	1834 ± 78	-78 ± 4	1396 ± 62
AuNP	-879 ± 83	$15\,731 \pm 1479$	-755 ± 190	$13\,514 \pm 3391$	-486 ± 55	8690 ± 992
Frag-Ab/AuNP ratio	1.16×10^3		1.38×10^3		1.63×10^3	

controllable AuNP adsorption. As Frag-Ab immobilization on AuNP modified surfaces was influenced by the amount of adsorbed AuNPs, the evaluation of the Frag-Ab surface density was challenging. For that reason, we decided to estimate Frag-Ab/AuNP ratios by dividing the amount of Frag-Ab by the amount of AuNPs. The amounts of Frag-Ab and AuNPs were calculated by dividing surface mass densities by the mass of a molecule or particle. The calculated ratios revealed the same tendency as in the case of Frag-Ab immobilization on planar Au surfaces. The highest Frag-Ab/AuNP ratio was 1.63×10^3 after immobilization from the antibody solution of $440 \mu\text{g mL}^{-1}$ and the lowest ratio of 1.16×10^3 was observed after the immobilization of Frag-Ab from the initial solution of $100 \mu\text{g mL}^{-1}$.

It is important to note that results obtained by QCM-D include not only the mass of the deposited proteins but also the mass of water bound *via* hydrogen bonds to the protein layer, the friction between the adsorbed structures and the solution and hydrodynamic resistance. The percentage of coupled water in protein layers is often higher than 75% and in some cases it can reach 98%.^{21–23} However, this parameter has not been addressed in the present study. In order to get more information on the water content of the investigated layers, the employment of additional independent methods (*e.g.*, optical) is required.

3.3 Frag-Ab and gp 51 interaction

After Frag-Ab immobilization on planar Au and AuNP modified surfaces and blocking the surface with 10 mg mL^{-1} BSA, the formation of the Frag-Ab complex with gp51 at $0.01\text{--}1 \text{ mg mL}^{-1}$ was evaluated. The response of Frag-Ab immobilized on planar Au and AuNP modified surfaces to 0.5 mg mL^{-1} gp51 *vs.* time is depicted in Fig. S2†.

In the case of a planar Au QCM-D sensor, the highest analytical signal was obtained on surfaces prepared from $100 \mu\text{g mL}^{-1}$ antibody solution (Fig. 2). As mentioned above, Frag-Ab immobilization from this solution also resulted in the lowest surface mass density of Frag-Ab (922 ng cm^{-2}).

The same tendency of Frag-Ab/gp51 interaction was observed on AuNP modified sensor surfaces. The highest analytical signal was registered in the system pre-modified with $100 \mu\text{g mL}^{-1}$ antibody solution with the smallest Frag-Ab/AuNP ratio of 1.16×10^3 . In this case the observed response was also the highest of all the investigated systems. When comparing planar Au and

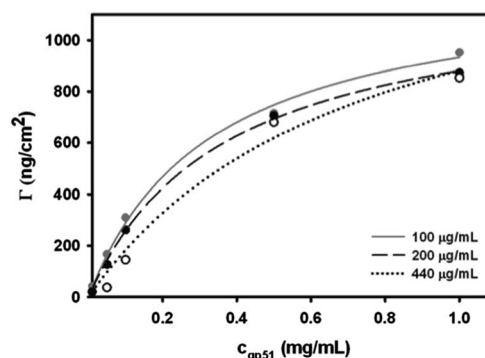


Fig. 2 Dependence of Frag-Ab/gp51 complex formation on the concentration of gp51 on planar Au electrode surfaces. Frag-Ab coated surfaces were prepared using Frag-Ab produced from different concentrations of antibody solution (100 , 200 or $440 \mu\text{g mL}^{-1}$).

AuNP modified sensor surfaces, the highest analytical signal was obtained in the AuNP based system formed from $100 \mu\text{g mL}^{-1}$ antibody solution (Fig. 3).

When solutions with higher initial antibody concentrations were investigated, the responses were similar on both planar Au and AuNP-based sensor surfaces. It is also interesting to note that the highest analytical signal obtained in the AuNP-based system differed significantly from the signals obtained on surfaces pre-modified with antibody solutions of higher initial

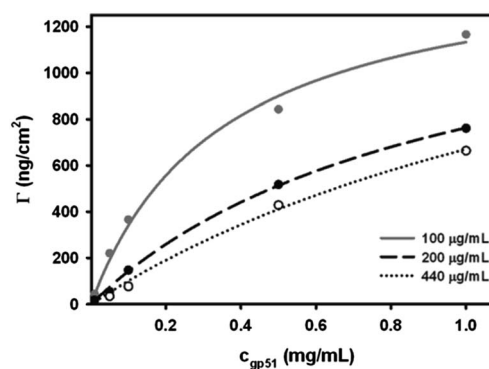


Fig. 3 Dependence of Frag-Ab/gp51 complex formation on the concentration of gp51 on AuNP modified Au electrode surfaces. Frag-Ab coated surfaces were prepared using Frag-Ab produced from different concentration antibody solutions (100 , 200 or $440 \mu\text{g mL}^{-1}$).

concentrations. In contrast, the differences between the surfaces pre-modified with antibody solutions of different concentrations on the planar Au QCM-D sensors were less distinctive.

Apparently steric hindrance plays a major role in Frag-Ab interactions with antigens. The increase in the response of the AuNP-based system after modification with Frag-Ab prepared from $100 \mu\text{g mL}^{-1}$ antibody solution indicated that when Frag-Ab molecules were less densely packed, a higher QCM-D response could be obtained. No significant differences in the planar Au-based systems were observed. These results could be influenced by redundant concentrations of Frag-Ab. It is likely that in tightly packaged Frag-Ab layers accessibility of the antigen binding sites to antigen gp51 was decreased due to steric hindrance.

3.4 Comparison of the specific gp51 interaction with Frag-Ab and its non-specific interaction with BSA

$\Delta D/\Delta f$ plots of QCM-D data (sometimes referred to as D - f plots) can be obtained by plotting Δf on the abscissa axis representing a mass increase (adsorption) on the surface and plotting ΔD on the ordinate axis illustrating changes in viscoelastic properties of the formed layer. Time is not plotted but its increase can be inferred by following the trace outwards from the origin. $\Delta D/\Delta f$ plots provide different kinds of information. Firstly, the adsorption kinetics can be evaluated by analysing the distance between the points of the plot. Points situated more adjacent to each other indicate slower kinetics than points that are more distant and reveal faster kinetics. Secondly, a change in the direction of the ΔD vs. Δf trace demonstrates the change of the process at the surface. Finally, the $\Delta D/\Delta f$ ratio represents the viscoelastic properties of the formed layer. A trace with a high $\Delta D/\Delta f$ ratio indicates that the adsorption process leads to the formation of a soft, flexible and viscous layer, while the trace with a low $\Delta D/\Delta f$ ratio indicates the formation of a firm and rigid material. It has been suggested that the D -factor changes are likely to be caused by the dynamic changes in protein layer, such as, changes in protein conformation, density, orientation, and hydration upon adsorption and by the trapped interlayer water effects since both these components contribute to energy loss.^{24,25} This, though qualitative, information is difficult to obtain by using other techniques.

In this study, gp51 interaction with Frag-Ab immobilized on planar Au and AuNP modified QCM-D sensor surfaces was compared with its non-specific interaction with BSA pre-adsorbed on planar Au and AuNP modified surfaces. The averaged Δf and ΔD values of three overtones (3rd, 5th, and 7th) obtained after exposing Frag-Ab (pre-formed from $100 \mu\text{g mL}^{-1}$ antibody solution) and BSA modified surfaces to 0.5 mg mL^{-1} gp51 solution were chosen for constructing $\Delta D/\Delta f$ plots. The analysis of these plots (Fig. 4) revealed that gp51 interactions with surface bound Frag-Ab or BSA adsorbed on planar Au surfaces showed distinguishably different $\Delta D/\Delta f$ traces. Fig. 4A represents the $\Delta D/\Delta f$ trace of Frag-Ab and gp51 interactions, while Fig. 4B shows the $\Delta D/\Delta f$ trace where only non-specific gp51 and BSA interactions are possible. The striking difference between the investigated $\Delta D/\Delta f$ traces was the rapid

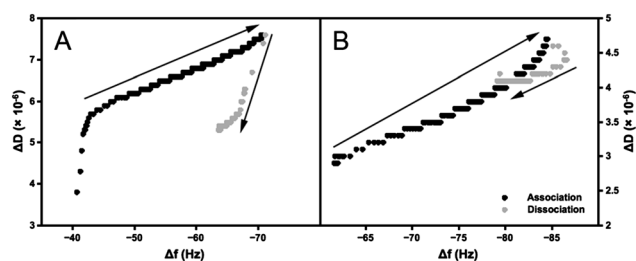


Fig. 4 $\Delta D/\Delta f$ dependence of immobilized Frag-Ab (A) and adsorbed BSA (B) on planar Au electrode surfaces in response to 0.5 mg mL^{-1} of gp51 solution in the QCM-D cell. Black points indicate ΔD vs. Δf for the association phase, while grey points indicate the dissociation phase, i.e., rinsing of gp51 with buffer. Arrows indicate the increase in time during the association and dissociation phases, respectively.

increase in dissipation at the initial stages of gp51 association (black points) and dissociation (grey points) at Frag-Ab modified surfaces (Fig. 4A). This $\Delta D/\Delta f$ trace feature was completely absent when gp51 interacted with the BSA modified surface (Fig. 4B). More specifically, two linear regimes could be observed in the Frag-Ab/gp51 trace, the initial one exhibiting a considerably higher slope than the following one. In contrast, only one linear regime was observed in the BSA/gp51 trace.

In the case of planar Au bound Frag-Ab/gp51 interaction, the high initial $\Delta D/\Delta f$ ratio indicated that at the initial stages of the reaction the forming protein layer was softer and more flexible in contrast to the following stage of the interaction that revealed the formation of a more rigid and stiff unyielding material. We suggest that the initial increase in the $\Delta D/\Delta f$ ratio of the Frag-Ab/gp51 interaction could be caused by two main processes. Firstly, the abrupt increase in dissipation could be influenced by molecular rearrangements in the surface-bound Frag-Ab layer upon interaction with antigens. It is known that antibodies are very flexible and adaptive molecules that change their conformation upon antigen binding. An antibody molecule can exhibit several different movements, for example, the Fab fragment is flexible about the hinge region for allowing a variable antigen reach and Fc wagging is employed to enable the attachment of the effector molecule.²⁶ In addition, since antibody-antigen interaction is based on a two-step induced fit mechanism, both antibody and antigen molecules undergo local conformational changes, such as, small movements of side-chains or structural modifications of the antibody CDR loops.²⁷ On the other hand, an abrupt increase in dissipation could reflect the forming complex in terms of interprotein interactions. Given the assumptions of Frag-Ab/gp51 binding at very localized epitope regions and no other multiple antigen-antibody interaction occurring that would restrict flexibility of the antigen-antibody couple, the high $\Delta D/\Delta f$ ratio can be interpreted as a result of an initial forming of flexible Frag-Ab/gp51 complexes.

The second linear regime exhibited a gradual $\Delta D/\Delta f$ slope revealing that the protein layer became more rigid and unyielding. This could be explained by an increase in multiple intermolecular interactions that resulted in a much stronger adsorbate-surface interaction, which stabilized the protein layer.

An abrupt increase in $\Delta D/\Delta f$ ratio during the dissociation phase (initial part of grey points, Fig. 4A) indicated that over the entire experiment there were molecules bound pliantly at the Frag-Ab modified surface. The presence of this molecule fraction might be essential for realising specific binding since localized and not stabilized by multiple bonding intermolecular interaction would allow easy rearrangements of the molecules at the surface and thus optimising the molecular orientation for specific antibody–antigen association.

In contrast, during the non-specific BSA/gp51 interaction on the planar Au surface (Fig. 4B), the increase in dissipation during the association phase was gradual from the initial stage. Dissociation accordingly resulted in a gradual decrease in dissipation. Such $\Delta D/\Delta f$ behaviour indicated that adsorbing molecules were possibly involved in multiple interactions and thus formed a more rigid adsorbate layer. Additionally, it might be that the growth of the rigid protein layer was due to a non-specific gp51 adsorption at the gold electrode surface, which was not covered by BSA. From $\Delta D/\Delta f$ data it is impossible to separate intermolecular forces driving the non-specific gp51 interaction with the BSA modified surface. However, it is definite that at the BSA-modified surface the flexibly surface-bound fraction of gp51 molecules was absent.

The same tendencies could be observed in the AuNP-based system. Specific Frag-Ab/gp51 interaction (Fig. 5A, black points) showed more abrupt changes in dissipation at the initial stages in comparison to the process at the surface, which allowed only non-specific BSA/gp51 interaction (Fig. 5B, grey points). The rinsing step resulted in a sudden decrease in dissipation at the beginning of the process at Frag-Ab modified surfaces in comparison to a gradual dissipation decrease in the case of the BSA-modified surface. From these experiments it can be concluded that qualitatively molecular gp51 interaction with Frag-Ab and BSA modified surfaces seems to be very similar in the cases of planar and nanostructured (AuNP-modified) gold surfaces.

Summarising $\Delta D/\Delta f$ plot analysis it can be concluded that $\Delta D/\Delta f$ plots revealed considerable differences between ΔD vs. Δf traces for the process governed by the gp51 interaction with surface bound Frag-Ab and by the non-specific gp51 interaction with the BSA modified surface. This qualitative analysis allows

us to propose that at Frag-Ab modified surfaces there are always some pliant Frag-Ab/gp51 complexes. These molecules should be reasonably mobile and thus enable rearrangements and orientations, which are required for realising specific antibody–antigen association. These our observations exploit and confirm previously formulated suggestions that examining the ΔD and Δf changes could not only be significant for representation and comparison of different processes but it could also indicate the structural alterations of individual proteins or within the protein layer during the adsorption, association and dissociation phases.^{17,25,28}

4. Conclusions

Site-directed Frag-Ab immobilization on planar Au and AuNP modified sensor surfaces and the resulting interaction with antigen gp51 were investigated by QCM-D. During the immobilization procedure antibodies were reduced in the hinge region by 2 ME to two identical “half” antibody fragments each having one antigen binding site and free sulfhydryl groups for attachment to the Au surface. Different concentrations of the initial antibody solutions were tested. Higher responses to gp51 were exhibited by Frag-Ab immobilized on AuNP modified surfaces in the range of all tested Frag-Ab concentrations. The lowest Frag-Ab surface mass densities resulted in the highest responses to gp51 on both types of surfaces, the best response being displayed by the AuNP modified sensor surface with a Frag-Ab/AuNP ratio of 1.16×10^3 . Specific and non-specific interactions were represented as QCM-D $\Delta D/\Delta f$ plots revealing distinct traces of Frag-Ab/gp51 and BSA/gp51 interactions.

Acknowledgements

The study was funded by the European Community's social foundation through the project “under Grant Agreement no. VP1-3.1-SMM-08-K-01-004/KS-120000-1756”. TR thanks The Swedish Research council for financial support.

References

- 1 A. Makaraviciute and A. Ramanaviciene, *Biosens. Bioelectron.*, 2013, **48**, 100–106.
- 2 A. Kausaite-Minkstimiene, A. Ramanaviciene, J. Kirlyte and A. Ramanavicius, *Anal. Chem.*, 2010, **82**, 6401.
- 3 Z. Balevicius, A. Ramanaviciene, I. Baleviciute, A. Makaraviciute, L. Mikoliunaite and A. Ramanavicius, *Sens. Actuators, B*, 2011, **160**, 555.
- 4 G. Bergstrom and C. F. Mandenius, *Sens. Actuators, B*, 2011, **158**, 265.
- 5 R. Elshafey, A. C. Tavares, M. Siaj and M. Zourob, *Biosens. Bioelectron.*, 2013, **48**, 100–106.
- 6 A. Lotfabad, H. Ghourchian and S. Kaboudanian Ardestani, *Anal. Bioanal. Electrochem.*, 2011, **3**, 450.
- 7 J. Baniukevic, I. Hakki Boyaci, A. Goktug Bozkurt, U. Tamer, A. Ramanavicius and A. Ramanaviciene, *Biosens. Bioelectron.*, 2013, **43**, 281.
- 8 R. G. Nuzzo, B. R. Zegarski and L. H. Dubois, *J. Am. Chem. Soc.*, 1987, **109**, 733.

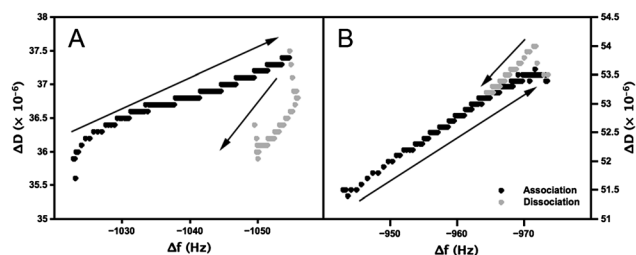


Fig. 5 $\Delta D/\Delta f$ dependence of immobilized Frag-Ab (A) and adsorbed BSA (B) on AuNP modified Au electrode surfaces in response to 0.5 mg mL^{-1} of gp51 solution in the QCM-D cell. Black points indicate ΔD vs. Δf for the association phase, while grey points indicate the dissociation phase, i.e., rinsing of gp51 with buffer. Arrows indicate the increase in time during the association and dissociation phases, respectively.

- 1 9 M. Shimizu, K. Kobayashi, H. Morii, K. Mitsui, W. Knoll and T. Nagamune, *Biochem. Biophys. Res. Commun.*, 2003, **310**, 606.
- 10 P. Roach, D. Farrar and C. C. Perry, *J. Am. Chem. Soc.*, 2006, **128**, 3939.
- 5 11 J. E. Gagner, M. D. Lopez, J. S. Dordick and R. W. Siegel, *Biomaterials*, 2011, **32**, 7241.
- 12 K. Bonroy, J.-M. Friedt, F. Frederix, W. Laureyn, S. Langerock, A. Campitelli, M. Sára, G. Borghs, B. Goddeeris and P. Declerck, *Anal. Chem.*, 2004, **76**, 4299.
- 10 13 D. Tang, B. Zhang, J. Tang, L. Hou and G. Chen, *Anal. Chem.*, 2013.
- 4 14 F. Salam, Y. Uludag and I. E. Tothill, *Talanta*.
- 15 R. Funari, B. Della Ventura, L. Schiavo, R. Esposito, C. Altucci and R. Velotta, *Anal. Chem.*, 2013, **85**, 6392.
- 15 16 M. Rodahl, F. Hook, A. Krozer, P. Brzezinski and B. Kasemo, *Rev. Sci. Instrum.*, 1995, **66**, 3924.
- 17 F. Höök, M. Rodahl, P. Brzezinski and B. Kasemo, *Langmuir*, 1998, **14**, 729.
- 20 18 J. Turkevich, P. C. Stevenson and J. Hillier, *Discuss. Faraday Soc.*, 1951, **11**, 55.
- 19 B. Ehresmann, P. Imbault and J. H. Well, *Anal. Biochem.*, 1973, **54**, 454.
- 20 A. A. Karyakin, G. V. Presnova, M. Y. Rubtsova and A. M. Egorov, *Anal. Chem.*, 2000, **72**, 3805.
- 21 H. Agheli, J. Malmström, E. M. Larsson, M. Textor and D. S. Sutherland, *Nano Lett.*, 2006, **6**, 1165.
- 5 22 G. Olanya, E. Thormann, I. Varga, R. Makuška and P. M. Claesson, *J. Colloid Interface Sci.*, 2010, **349**, 265.
- 23 J. Rickert, A. Brecht and W. Göpel, *Biosens. Bioelectron.*, 1997, **12**, 567.
- 10 24 G. Mccubbin, S. Praporski, S. Piantavigna, D. Knappe, R. Hoffmann, J. Bowie, F. Separovic and L. Martin, *European Biophysics Journal*, 2011, **40**, 437.
- 25 D. E. Otzen, M. Oliveberg and F. Höök, *Colloids Surf., B*, 2003, **29**, 67.
- 15 26 D. R. Burton, *Trends Biochem. Sci.*, 1990, **15**, 64.
- 27 I. Kumagai and K. Tsumoto, in *Els*, John Wiley & Sons, Ltd, 2001.
- 20 28 F. Höök, M. Rodahl, B. Kasemo and P. Brzezinski, *Proc. Natl. Acad. Sci.*, 1998, **95**, 12271.
- 25
- 30
- 35
- 40
- 45
- 50
- 55